X. ELECTRONIC SPECTROSCOPY

1. Rovibronic energy levels

In §§ VIII and IX, we considered transitions between vibration-rotation levels within the ground electronic state. As we have seen in §VII, however, a molecule also has an (infinite) number of excited electronic states. Consider for simplicity a diatomic molecule. For each excited electronic state, there is a potential energy curve, and for bound states, the curve appears qualitatively similar to that of the ground state. However, as we have seen for the case of H_2 and H_2^+, some potential curves can be unbound or repulsive.

In spectroscopy, generally only transitions between a bound upper electronic state and a bound lower state are observed. Such a transition involves simultaneous changes in the vibrational and rotational energy levels. For each state, the energy or spectroscopic term can be written as

$$E \quad = \quad T_e + G_v + F_v(J). \tag{10.1}$$

The electronic term T_e measures the energy of the minimum of the potential curve for a particular state above the minimum of the ground state curve. For the ground state itself, $T_e = 0$. If the energies were measured with respect to the separated atoms, $T_e = -D_e$ for the ground state, but it is not customary to do so. The vibrational terms G_v are given by the expressions in § IX; the rotational term values $F_v(J)$ in §VIII. The actual spectrum consists of a large number of lines with frequencies

$$h\nu \quad = \quad (T_e' - T_e'') + G_{v'} + F_{v'}(J) - G_{v''} - F_{v''}(J). \tag{10.2}$$

Vibrational transitions accompanying an electronic transition are called "vibronic" transitions. The vibronic transitions and their accompanying rotational, or so-called "rovibronic" transitions, are group into bands in the spectrum, and the set of bands associated with a single electronic transition is called an electronic "band system".

2. Selection rules; the Franck-Condon principle

As for vibrational and rotational transitions, the strength of an electronic transition is proportional to the square of the matrix element between the upper and lower state:

$$\vec{R} = < \Psi' | \vec{d} | \Psi'' > = \int \Psi'^* \vec{d} \Psi'' d(\vec{r}\vec{R}) \tag{10.3}$$

where

$$\vec{d} = \vec{d}^{el} + \vec{d}^{nuc} = -\sum_i \vec{r}_i + \sum_\alpha Z_\alpha \vec{R}_\alpha \tag{10.4}$$

is the electric dipole operator, and the integration in (10.3) is over both the electronic and the nuclear coordinates. In the Born-Oppenheimer approximation, we obtain (neglecting rotation for simplicity):

$$< e'v' | \vec{d} | e''v'' > = < v' < e' | \vec{d}^{el} + \vec{d}^{nuc} | e'' > v'' >$$

$$= < v' < e' | \vec{d}^{el} | e'' > v'' > + < e' | e'' > < v' | \vec{d}^{nuc} | v'' > . \tag{10.5}$$

The second term of (10.5) vanishes, because the set of electronic wave functions is orthonormal. If the electronic transition dipole moment is defined as

$$D^{el}(R) =< e'|\vec{d}^{el}|e'' > \tag{10.6}$$

then

$$\vec{R} =< v'|D^{el}(R)|v'' >= \int \Psi^{v'*}(R) D^{el}(R) \Psi^{v''}(R) dR \tag{10.7}$$

where the integration in (10.7) is over the nuclear coordinates only. If D^{el} varies little with R in the vicinity of the equilibrium internuclear coordinates,

$$D^{el}(R) \approx D^{el}(R_e), \tag{10.8}$$

then it can be taken out of the integral, so that we obtain

$$\vec{R} = D^{el}(R_e) < v'|v'' > \tag{10.9}$$

The oscillator strength for the transition then becomes

$$f_{v'v''} = \frac{2}{3} \cdot g|D^{el}(R_e)|^2| < v'|v'' > |^2 \Delta E_{v'v''} \tag{10.10}$$

if both the transition dipole moment and the energy difference $\Delta E_{v'v''}$ are expressed in atomic units. Here g is a degeneracy factor equal to

$$g = \frac{2 - \delta_{\Lambda' + \Lambda''}}{2 - \delta_{\Lambda''}} \tag{10.11}$$

for a diatomic molecule. The corresponding Einstein A-coefficient

$$A_{v'v''} = \frac{2}{3} \cdot \frac{2 - \delta_{\Lambda' + \Lambda''}}{2 - \delta_{\Lambda''}} \tilde{\nu}^2 f_{v'v''}$$

$$= 2.03 \times 10^{-6} \frac{2 - \delta_{\Lambda' + \Lambda''}}{2 - \delta_{\Lambda''}} \tilde{\nu}^3 |D^{el}(R_e)|^2| < v'|v'' > |^2 \tag{10.12}$$

if $\tilde{\nu}$ is the transition frequency in wavenumbers. Thus, the relative intensity of a transition between any two vibrational states is given by the square of the "vibrational overlap integral"

$$q_{v'v''} = | < v'|v'' > |^2 \tag{10.13}$$

which is known as the "Franck-Condon factor." The following sum rule holds for the Franck-Condon factors

$$\sum_{v''} q_{v'v''} = \sum_{v''} < v'|v'' >< v''|v' >=< v'|v' >= 1 \tag{10.14}$$

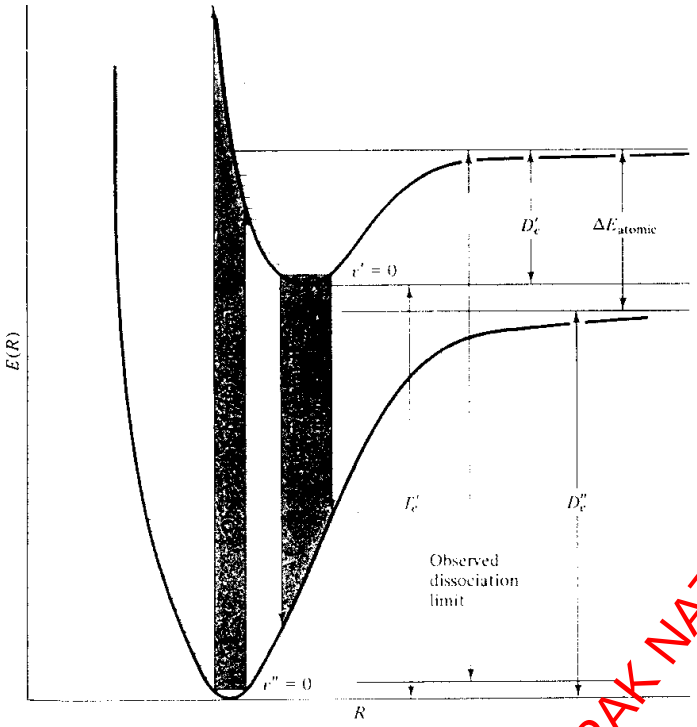

Figure 10.1– The "vertical transitions permitted by the Franck-Condon principle between two electronic states. Also shown schematically is the relation among the dissociation energy of the ground state, D''_e, that of the excited state, D'_e, and the electronic term T'_e.

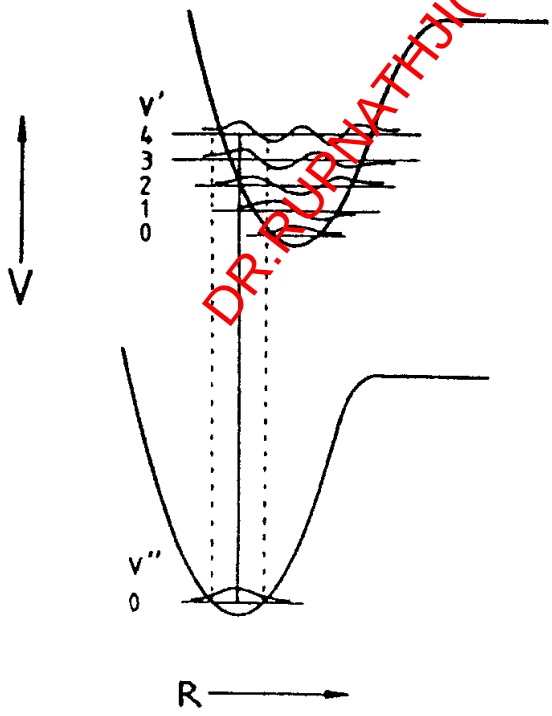

Figure 10.2– The Franck-Condon principle applied to a case in which $R'_e > R''_e$ and the (4,0) transition is the most probable.

where we have used the completeness relation

$$\sum_{v''} |v'' >< v''| = 1. \tag{10.15}$$

The physical interpretation of the Franck-Condon factor is consistent with the original basis of the Born-Oppenheimer separation, namely that the nuclei are moving much more slowly than the electrons. It says that in the 'time' required for an electronic transition to occur, which is of order $h/\Delta E \approx 10^{-14}$s, the nuclei do not move. Thus, the band with the highest transition probability is the one for which the transition is "vertical", that is, the molecule finds itself in the excited electronic state with the same internuclear separation as it had in the ground electronic state.

This is illustrated in Figure 10.1 for the case of a diatomic molecule. The only regions of the excited state potential that are accessible in the transition are those for which the vibrational wave function of the ground state has a finite value. An analogous argument holds for emission spectra. Note that if the vibrational wavefunctions $\Psi^{v'}$ and $\Psi^{v''}$ have several nodes, there will be interference effects, leading to irregular variations in the Franck-Condon factors. For higher v, the maximum contribution comes from the part of the wave function closest to the classical turning point, as Figure 10.2 shows. The solid line in this figure indicates the maximum contribution to the vibrational overlap integral, which occurs in this example for v'=4. Clearly, the overlap integrals for v' close to 4 are also appreciable, however, and give an intensity distribution like that illustrated in Figure 10.3b. Such an intensity distribution is called a "progression"; it involves a series of vibronic transitions with a common lower or upper levels. In this example, all members of the progression have v''=0 in common. A group of transitions with the same value of Δv is referred to as a "sequence".

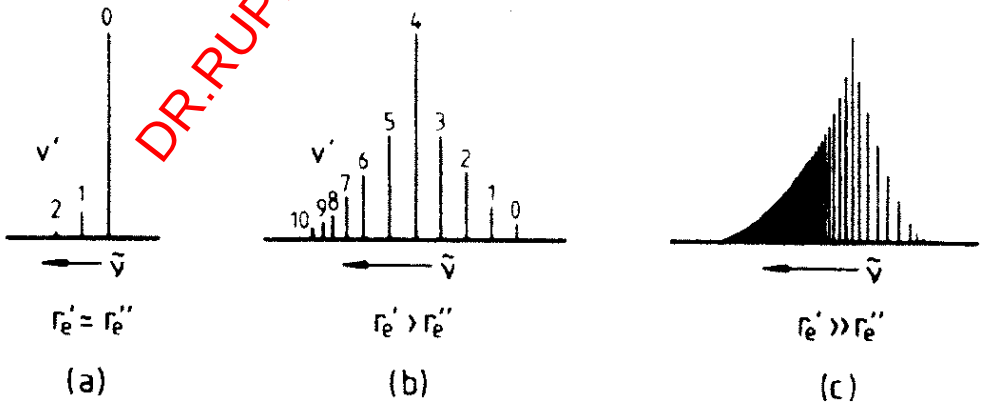

Figure 10.3– Typical vibrational progressions and intensity distributions for the cases $R'_e \approx R''_e$, $R'_e > R''_e$, $R'_e \gg R''_e$.

The situation illustrated in Figure 10.2 and 10.3b arises when $R'_e > R''_e$, that is, the equilibrium internuclear distance in the upper state is larger than that in the ground state. This is usually the case, since the ground state has the strongest bonding. Figure 10.3a

shows the expected spectrum in the case $R'_e \approx R''_e$. The maximum intensity occurs for the (0,0) band, and it falls off very rapidly. Very occasionally, the situation occurs in which $R'_e < R''_e$, although it usually only arises in transitions between two excited electronic states. The result is again an intensity distribution like that in Figure 10.3b, so that an observation of a long $v'' = 0$ progression with an intensity maximum at $v' > 0$ indicates qualitatively an appreciable change in R_e from the lower to the upper state, but does not indicate the sign of the change. However, if anharmonicity is considered, there will be some slight differences between the two cases. For $R'_e > R''_e$, the relatively steep part of the excited state potential curve above v''=0 is sampled, giving rise to a relatively broad maximum in the progression intensity. For $R'_e < R''_e$, the shallower part of the excited state potential curve is probed, resulting in a sharper intensity distribution. If $R'_e >> R''_e$, appreciable intensity may arise from absorption into the continuum of vibrational levels above the dissociation limit, as illustrated in Figure 10.3c.

The selection rules for the electronic states involved in an electric dipole transition can be derived using group theory, as explained in § VII. The requirement is that the product of the symmetry types of the lower and upper state wave functions, and that of the dipole moment operator is totally symmetric:

$$\Gamma(\Psi_u^{el}) \times \Gamma(\vec{d}^{el}) \times \Gamma(\Psi_g^{el}) = A_1. \tag{10.16}$$

For diatomic molecules, this results in the following selection rules:

$$\Delta\Lambda = 0, \pm 1$$

$$\Delta S = 0. \tag{10.17}$$

Also, for sigma states, we find $\Sigma^+ \leftrightarrow \Sigma^+$, $\Sigma^- \leftrightarrow \Sigma^-$, but $\Sigma^+ \not\leftrightarrow \Sigma^-$. For homonuclear species, we have the additional rule $g \leftrightarrow u$, but $g \not\leftrightarrow g$ and $u \not\leftrightarrow u$.

For completeness, the selection rules for the higher order transitions are:

Magnetic Dipole:
$\Delta\Lambda = 0, \pm 1$
$\Delta S = 0^*$
$\Sigma^+ \not\leftrightarrow \Sigma^+$, $\Sigma^- \not\leftrightarrow \Sigma^-$, $\Sigma^+ \leftrightarrow \Sigma^-$
$g \leftrightarrow g$, $u \leftrightarrow u$, $g \not\leftrightarrow u$

Electric Quadrupole:
$\Delta\Lambda = 0, \pm 1, \pm 2$
$\Delta S = 0^*$
$\Sigma^+ \leftrightarrow \Sigma^+$, $\Sigma^- \leftrightarrow \Sigma^-$, $\Sigma^+ \not\leftrightarrow \Sigma^-$
$u \leftrightarrow u$, $g \leftrightarrow g$, $g \not\leftrightarrow u$

*In both cases the ΔS=0 rule will break down to the extent that spin-orbit coupling occurs.

3. Examples

a) O_2

Figure 10.4 illustrates some of the potential energy curves of the O_2 molecule. It is clear that there are a large number of electronic states at relatively low energies. Most of these states dissociate into ground state atoms $O(^3P)$ + $O(^3P)$. Conversely, these atoms give rise to a whole suite of distinct molecular states. The symmetries of the molecular states can be found by adding the angular momentum of the separated atoms, and by projecting the result onto the internuclear axis. Thus, it is clear that two triplet states can give rise to singlet, triplet and quintet states, and that two P atoms with $L = 1$ can result in Λ=0, 1 and 2 (Σ, Π and Δ) states. Just as for atoms, the fact that the two ^3P states are equivalent excludes some combinations (such as the $^5\Delta_u$ state), but quite a number of possibilities remain. Such considerations of the possible electronic states correlating with the separated atoms are very useful, because they can be used to predict the presence of electronic states that have not yet been observed spectroscopically, especially the repulsive states. Such states are indicated with dashed lines in Figure 10.4. Tables of electronic states correlating with separated atoms can be found in Herzberg Vol. I, and are reproduced here in Tables 10.1 and 10.2.

The ground electronic state of O_2 has $^3\Sigma_g^-$ symmetry. Thus, electric dipole allowed transitions are possible to states of $^3\Sigma_g^-$ and $^3\Pi_g$ symmetry. The lowest electric-dipole allowed transition is the B $^3\Sigma_u^-$–X $^3\Sigma_g^-$ transition. As Figure 10.4 shows, the B $^3\Sigma_u^-$ potential curve is displaced to larger internuclear distances compared with the X $^3\Sigma_g^-$ curve, thus giving rise to a long progression from 2000-1750 Å. These are the so-called "Schumann-Runge bands." Above 1750 Å, the molecule can dissociate into $O(^3P)$ and $O(^1D)$, so that the absorption becomes continuous. This is called the "Schumann-Runge continuum." Figure 10.6 illustrates the absorption spectrum of the molecule at low spectral resolution. Both the Schumann-Runge bands and the continuum play an important role in the Earth's atmosphere.

At low energies (λ >2000 Å), a weak continuum is observed, which can be ascribed to the forbidden A $^3\Sigma_u^+$–X $^3\Sigma_g^-$ transition, and is called the Herzberg I system. The transition occurs by magnetic dipole radiation. Other forbidden transitions which are observed in the Earth's atmosphere are given in Figure 10.5. At high energies, λ <1300 Å, the absorption occurs into high-lying Rydberg states such as the 2 $^3\Sigma_u^-$ state. The ionization potential of O_2 is 12.06 eV, so that absorption at λ <1030 Å gives rise to the ionization continuum.

b) CH

Another interesting example is provided by the CH molecule, for which the potential energy curves are illustrated in Figure 10.7. The ground electronic state has $^2\Pi$ symmetry, so that electric dipole allowed transitions are possible to states of $^2\Sigma^+$, $^2\Sigma^-$, $^2\Pi$ and $^2\Delta$ symmetries. Lines of CH in the A $^2\Delta$–X $^2\Pi$, B $^2\Sigma^-$–X $^2\Pi$ and C $^2\Sigma^+$–X $^2\Pi$(0,0) systems have been observed in diffuse interstellar clouds in absorption against bright background stars. CH was, together with CH^+ and CN, one of the first interstellar molecules discovered at the end of the 1930's by such optical absorption methods. Similar absorption lines of CH^+ in the A $^1\Pi$–X $^1\Sigma^+$(0,0) band at 4232 Å, and of CN in the B $^2\Sigma^+$–X $^2\Sigma^+$ (0,0) band at 3874 Å have been seen (see Figure 10.8).

Table 10.1– Molecular Electronic States Resulting from Identical States of the Separated Like Atoms

States of the Separated Atoms*	Molecular States
$^1S + {}^1S$	$^1\Sigma_g^+$
$^2S + {}^2S$	$^1\Sigma_g^+, {}^3\Sigma_u^+$
$^3S + {}^3S$	$^1\Sigma_g^+, {}^3\Sigma_u^+, {}^5\Sigma_g^+$
$^4S + {}^4S$	$^1\Sigma_g^+, {}^3\Sigma_u^+, {}^5\Sigma_g^+, {}^7\Sigma_u^+$
$^1P + {}^1P$	$^1\Sigma_g^+(2), {}^1\Sigma_u^-, {}^1\Pi_g, {}^1\Pi_u, {}^1\Delta_g$
$^2P + {}^2P$	$^1\Sigma_g^+(2), {}^1\Sigma_u^-, {}^1\Pi_g, {}^1\Pi_u, {}^1\Delta_g, {}^3\Sigma_u^+(2), {}^3\Sigma_g^-, {}^3\Pi_g, {}^3\Pi_u, {}^3\Delta_u$
$^3P + {}^3P$	Singlet and triplet terms as for $^2P + {}^2P$; in addition, $^5\Sigma_g^+(2), {}^5\Sigma_u^-, {}^5\Pi_g, {}^5\Pi_u, {}^5\Delta_g$
$^1D + {}^1D$	$^1\Sigma_g^+(3), {}^1\Sigma_u^-(2), {}^1\Pi_g(2), {}^1\Pi_u(2), {}^1\Delta_g(2), {}^1\Delta_u, {}^1\Phi_g, {}^1\Phi_u, {}^1\Gamma_g$
$^2D + {}^2D$	Singlets as for $^1D + {}^1D$; in addition, $^3\Sigma_u^+(3), {}^3\Sigma_g^-(2), {}^3\Pi_u(2), {}^3\Pi_g(2), {}^3\Delta_u(2), {}^3\Delta_g, {}^3\Phi_u, {}^3\Phi_g, {}^3\Gamma_u$
$^3D + {}^3D$	Singlets as for $^1D + {}^1D$, triplets as for $^2D + {}^2D$, and quintets like singlets

* Whether the atomic state is even or odd is of no importance here, since both atoms are in the same state.

Table 10.2– Molecular Electronic States Resulting from Given States of the Separated (Unlike) Atoms

States of the Separated Atoms	Molecular States
$S_g + S_g$ or $S_u + S_u$	Σ^+
$S_g + S_u$	Σ^-
$S_g + P_g$ or $S_u + P_u$	Σ^-, Π
$S_g + P_u$ or $S_u + P_g$	Σ^+, Π
$S_g + D_g$ or $S_u + D_u$	Σ^+, Π, Δ
$S_g + D_u$ or $S_u + D_g$	Σ^-, Π, Δ
$S_g + F_g$ or $S_u + F_u$	$\Sigma^-, \Pi, \Delta, \Phi$
$S_g + F_u$ or $S_u + F_g$	$\Sigma^+, \Pi, \Delta, \Phi$
$P_g + P_g$ or $P_u + P_u$	$\Sigma^+(2), \Sigma^-, \Pi(2), \Delta$
$P_g + P_u$	$\Sigma^+, \Sigma^-(2), \Pi(2), \Delta$
$P_g + D_g$ or $P_u + D_u$	$\Sigma^+, \Sigma^-(2), \Pi(3), \Delta(2), \Phi$
$P_g + D_u$ or $P_u + D_g$	$\Sigma^+(2), \Sigma^-, \Pi(3), \Delta(2), \Phi$
$P_g + F_g$ or $P_u + F_u$	$\Sigma^+(2), \Sigma^-, \Pi(3), \Delta(3), \Phi(2), \Gamma$
$P_g + F_u$ or $P_u + F_g$	$\Sigma^+, \Sigma^-(2), \Pi(3), \Delta(3), \Phi(2), \Gamma$
$D_g + D_g$ or $D_u + D_u$	$\Sigma^+(3), \Sigma^-(2), \Pi(4), \Delta(3), \Phi(2), \Gamma$
$D_g + D_u$	$\Sigma^+(2), \Sigma^-(3), \Pi(4), \Delta(3), \Phi(2), \Gamma$
$D_g + F_g$ or $D_u + F_u$	$\Sigma^+(2), \Sigma^-(3), \Pi(5), \Delta(4), \Phi(3), \Gamma(2), H$
$D_g + F_u$ or $D_u + F_g$	$\Sigma^+(3), \Sigma^-(2), \Pi(5), \Delta(4), \Phi(3), \Gamma(2), H$

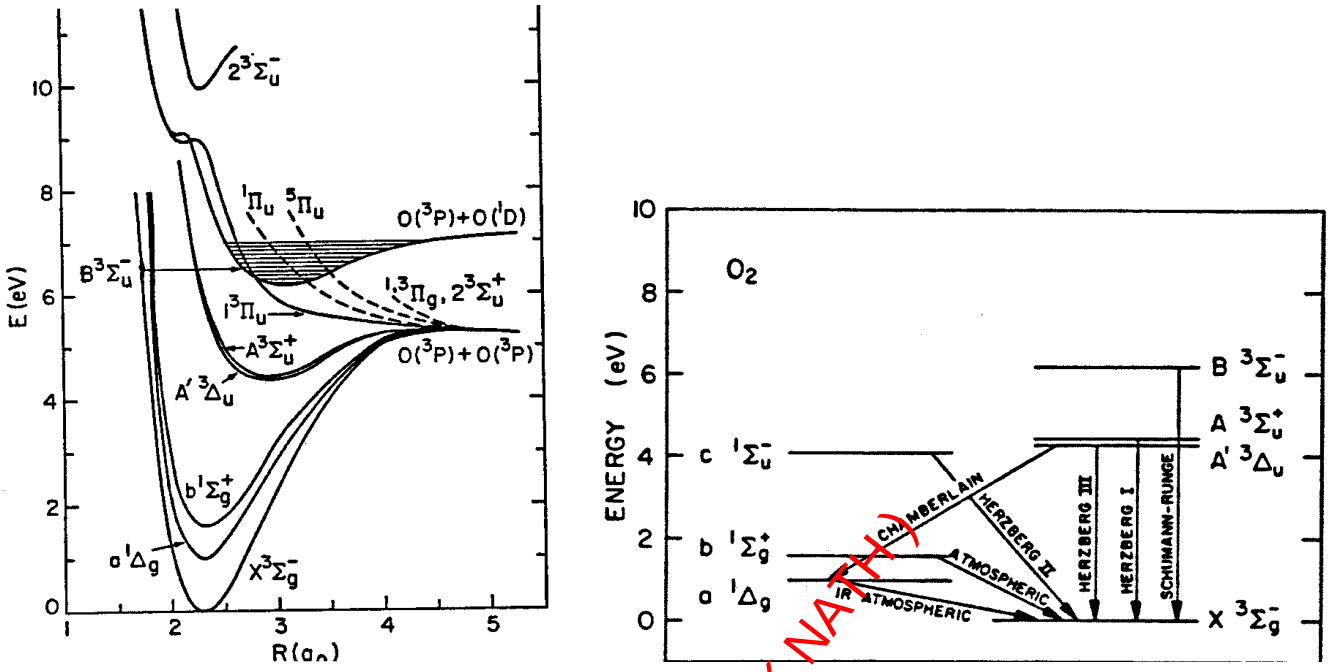

Figure 10.4– (Left) Potential energy curves for the low-lying electronic states of O_2.
Figure 10.5– (Right) Energy level diagram for O_2, showing transitions important in atmospheric airglow spectra.

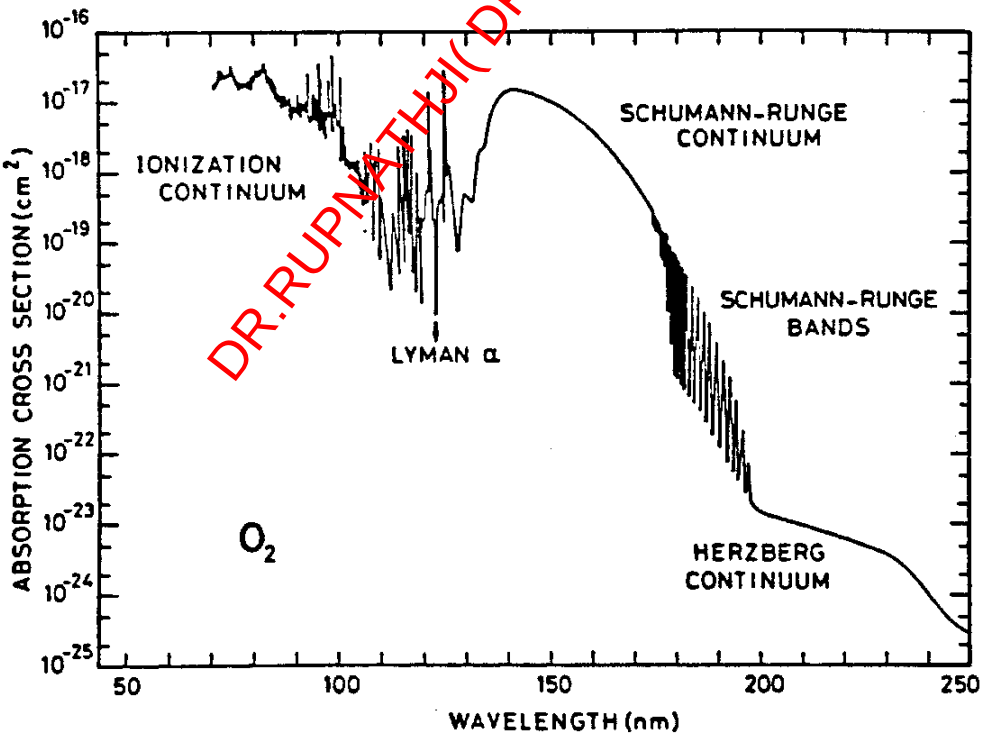

Figure 10.6– The UV absorption spectrum of O_2 at low resolution.

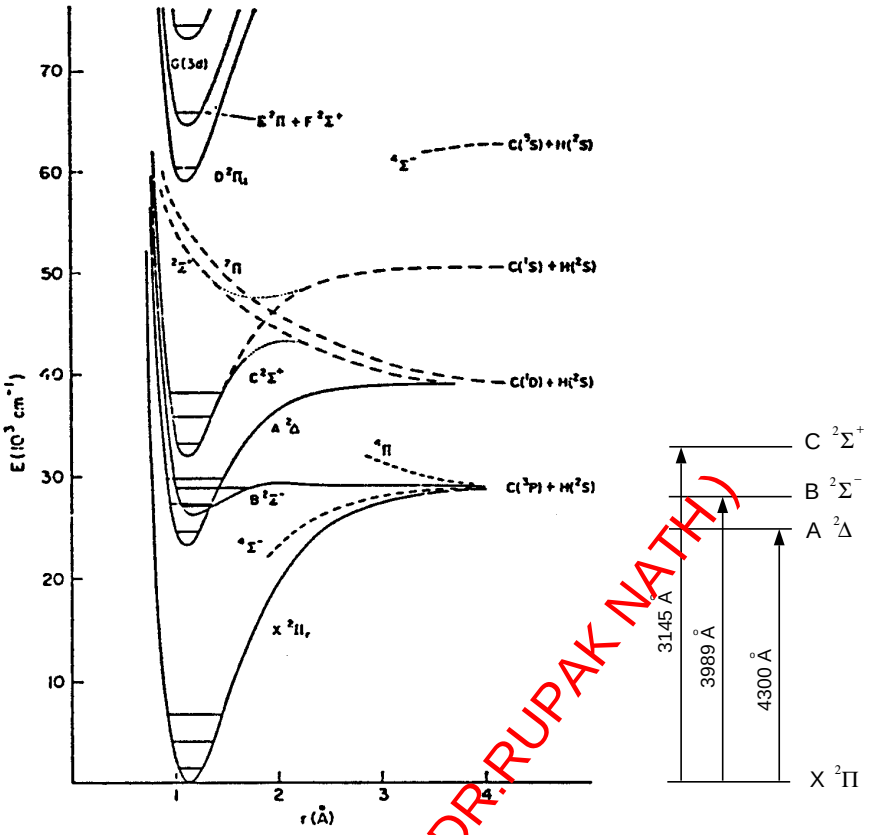

Figure 10.7– Potential curves of the known electronic states of CH. The higher Rydberg states are not included (from Herzberg & Johns 1969, *Ap. J.* **158**, 399).

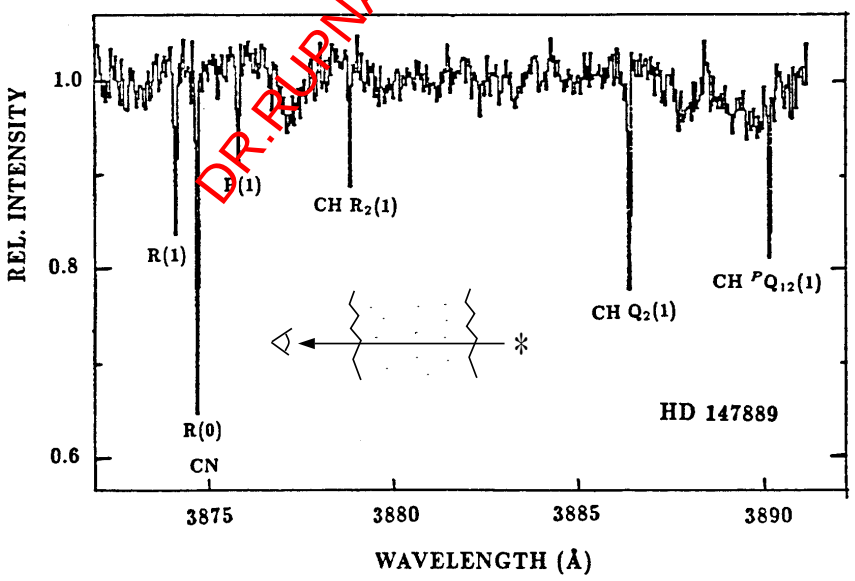

Figure 10.8– The observed absorption spectrum of the CH and CN A ← X transitions toward HD 147889.

4. Rotational structure of electronic transitions

Associated with the upper and lower vibronic states are sets of rotational levels, which give rise to rotational fine structure in the observed spectra. This structure is very similar to that found in the infrared vibrational transitions, except that a wider range of symmetry types can be involved. For simplicity, we will consider here only the structure of a $^1\Sigma$–$^1\Sigma$ transition in a diatomic molecule.

Figure 10.9 shows the rotational energy levels associated with two $^1\Sigma^+$ electronic states. The spectroscopic term of each of the states is given by (10.1) where

$$F_v(J) = B_v J(J+1) - D_v J^2(J+1)^2. \tag{10.18}$$

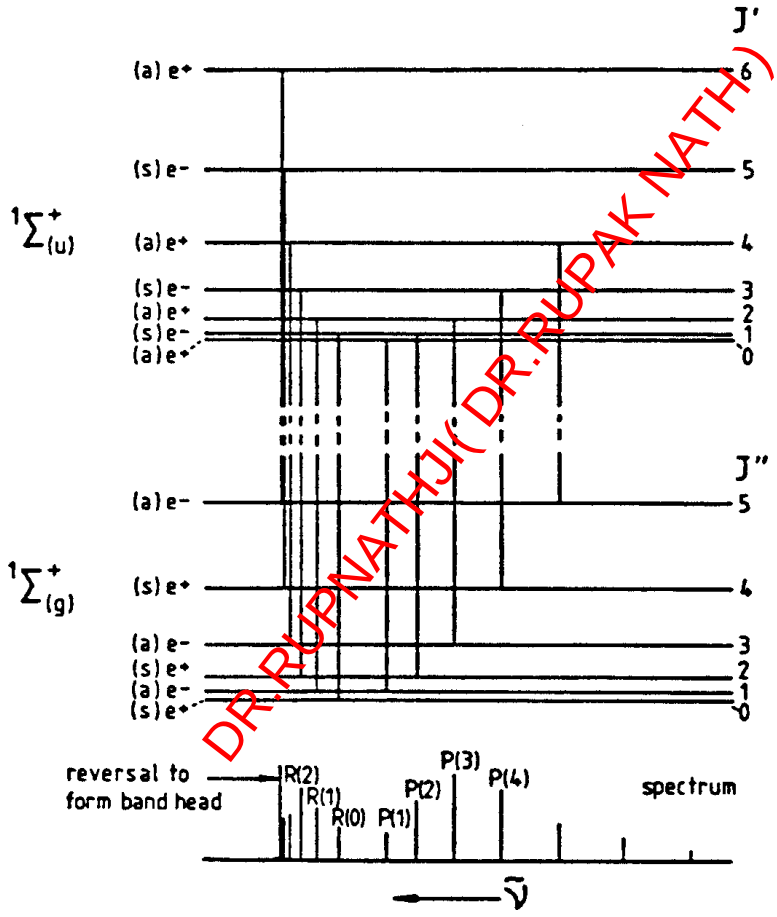

Figure 10.9– Rotational fine structure of a $^1\Sigma^+$ - $^1\Sigma^+$ electronic or vibronic transition in a diatomic molecule for which $r'_e > r''_e$. The g and u subscripts and the s and a labels apply only to a homonuclear diatomic molecule: the +, −, e, and f labels can be ignored.

Just as for vibration-rotation transitions, the selection rule is $\Delta J = \pm 1$, resulting in P-branch (ΔJ=–1) and R-branch (ΔJ=+1) structure. If one of the electronic states has $\Lambda > 0$, a Q-branch (ΔJ=0) occurs as well. Thus, we expect the band to look very similar to the v=1-0 infrared band of HCl (Figure 9.2), or the 3^1_0 band of HCN (Figure 9.8), as summarized in Figure 10.10.

In practice, however, the electronic ro-vibronic bands are very asymmetrical about the band center $\tilde{\nu}_0$ (which is defined as always as the wave number at which the utterly forbidden $J' = 0 - J'' = 0$ transition would occur). The reason for the asymmetry is that the rotational constants B' and B'' are typically very different in different electronic states, whereas they are very similar in different vibrational states within the same electronic state. Since most likely $R'_e > R''_e$, $B' < B''$. This means that the rotational levels diverge more slowly in the upper state than in the lower state. The spectrum at the bottom of Figure 10.9 has been drawn for this case, as has the spectrum at the top of Figure 10.11. A quantitative example for the I_2 molecule is shown in Figure 10.12. The result is a very asymmetric branch with a so-called "band head" in which the low J lines in the R branch run together. This is due to the fact that the R-branch shows a reversal, that is, for low J the lines lie to the blue of the band center, but for high J, they lie to the red. The P-branch lines lie to the red for all J in this example. Such a band is said to be "degraded", or "shaded", to the red, that is, to lower wave number. If $B' > B''$, the P-branch forms a head, and the band is degraded to the blue.

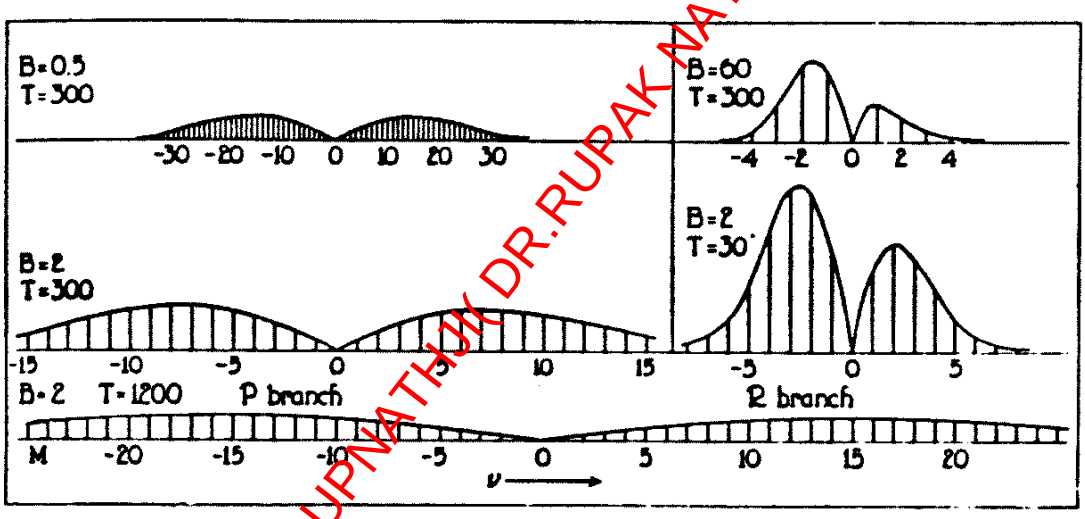

Figure 10.10– An illustration of the effect of the numerical values of B and T on the structure and intensity distribution for electronic emission or absorption bands having $B' \approx B''$ (headless bands). All the diagrams are on the same scale, except for the case $B = 60$ which is scaled by 25%.

The J value at which the branch turns around can be found by treating the line frequency

$$\tilde{\nu}_R(J) = \tilde{\nu}_0 + 2B' + (3B' - B'')J + (B'B'')J^2 \tag{10.19}$$

as a continuous variable, and differentiating it with respect to J:

$$\frac{d\tilde{\nu}_R(J)}{dJ} = (3B' - B'') + 2(B' - B'')J = 0$$

$$\Rightarrow J_R^* = -\frac{3B' - B''}{2(B' - B'')} \tag{10.20}$$

where J_R^* is the nearest integer value to this ratio of B-values.

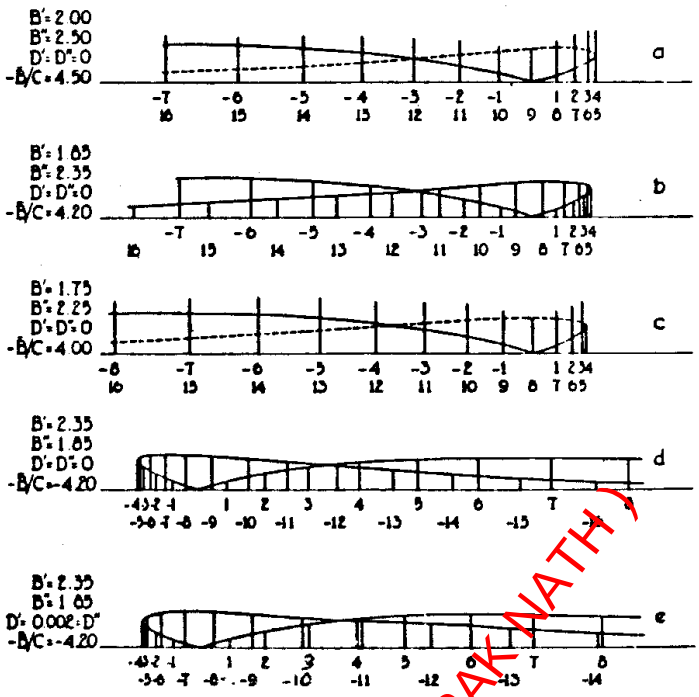

Figure 10.11 (Top three) Three illustrations of bands for which $B' < B''$, with associated R-branch band head formation. Frequency increases to the right, and so these bands are shaded to the red. (Bottom two) Here $B' > B''$, and so a P-branch band head is formed. Such bands are said to shade to the blue (or violet).

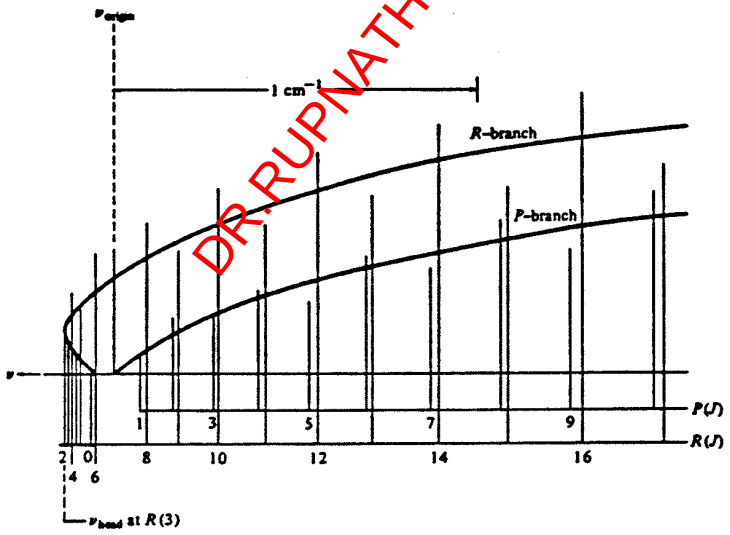

Figure 10.12 Band head formation in the 0-0 band of the iodine $B \rightarrow X$ transition. The intensity distribution shown corresponds to room temperature, and frequency increases to the left. Thus the band is "red shaded." The 7:5 nuclear spin intensity alteration is also included.

In general, the spontaneous transition probability for a single rotational line (that is, a transition connecting a single Λ sublevel spin-multiplet component for angular momentum quantum number J in a specific v-level of electronic state e with a sublevel of another electronic state):

$$A^{e'v'J's'p'}_{e''v''J''s''p''} = 2.03 \times 10^{-6} \frac{2 - \delta_{0,\Lambda'+\Lambda''}}{2 - \delta_{0,\Lambda'}} \tilde{\nu}^3 | < e'v' | D^{el}(R) | e''v'' > |^2 \frac{S_{J'J''}}{2J' + 1} \qquad (10.21)$$

where $S_{J'J''}$ is a "rotational line strength factor" for the line component $J's'p' \leftrightarrow J''s''p''$ and s and p designate the spin-multiplet and Λ-parity sublevels. It is easy to come to grief (usually by exactly factors of 2) in normalizing these line-strength factors; the proper normalization is

$$\sum_{s'} \sum_{p'} \sum_{J'} S_{J'J''} = (2 - \delta_{0,\Lambda'+\Lambda''})(2J'' + 1)(2S'' + 1) \qquad (10.22)$$

and similarly for summations over the double-primed quantum states. The absorption oscillator strength for a line is then given by:

$$f_{J'J''} = \frac{3}{2} \frac{2 - \delta_{0,\Lambda'}}{2 - \delta_{0,\Lambda''}} \tilde{\nu}^{-2} \left(\frac{2J'' + 1}{2J' + 1} \right) A^{e'v'J's'p'}_{e''v''J''s''p''}. \qquad (10.23)$$

A clear summary of many of these confusing points is given by Larsson 1983, *Astr. Ap.* **128**, 291, which is based upon more extensive discussions by: Whiting & Nicholls 1974, *Ap. J. Suppl.* **27**, 1. Schadee 1978, *J.Q.S.R.T.* **19**, 451. Whiting *et al.* 1980, *J. Mol. Spectrosc.* **80**, 249.

5. Electronic Spectroscopy of Polyatomic Molecules

The electronic spectra of polyatomic molecules can become hopelessly congested at high resolution because of the very high density of eigenstates. Furthermore, a sometimes bewildering array of radiative and non-radiative processes become important. Before turning to the spectroscopy of formaldehyde as an example of of some of the more important "rules" of polyatomic electronic spectroscopy, we first present a brief tabulation of terms:

I. A Brief Glossary of Terms in Electronic Spectroscopy

A. Absorption and Emission

Bound State-Bound State Transitions:
- Fluorescence – Spin allowed, $\tau \lesssim 10^{-7}$ sec
- Phosphorescence – Spin forbidden, $\tau \gtrsim 10^{-6}$ sec
- Raman effects – Spontaneous, resonant, stimulated
- Franck-Condon factors

Bound-Free Transitions (more next week):
- Photoioinization – resonant, non-resonant, pulsed field
- Photodissociation – direct, predissociation, coupled states, excimers . .
- The Reflection approximation and the Mulliken difference potential

B. Non-radiative Transitions

Predissociation (curve crossing)

Yablonski diagrams – internal conversion (IC), intersystem crossing (ISC), intermolecular vibrational redistribution (IVR), inverse electronic relaxation (IER), ...

C. Popular Experimental Techniques

Laser Induced Fluorescence:
- Excitation spectra (tune laser, measure total yield)
- Dispersed fluorescence (fix laser, disperse emission w/gratings, prisms,...)

Stimulated emission pumping (SEP, including four-wave mixing)

Photoelectron spectroscopy (lasers & mass spectrometers)

Multi-photon dissociation (MPD) & ionization (REMPI)

Picosecond/femtosecond pulses (pump-probe, CARS, ionization...)

We'll now look at some of these processes using H_2CO as a test case.

Formaldehyde: A Quick Rovibrational Review

As the figure below reminds you, formaldehyde is a four atom non-linear molecule. The point group to which it belongs is C_{2v}, and it is a nearly prolate top with an asymmetry parameter near -1. The permanent dipole moment is directed along the a-axis.

Since it is non-linear, there are 3(4)-6 = 6 *non-degenerate* normal modes of vibration. In the order derived by G. Herzberg, these six modes are:

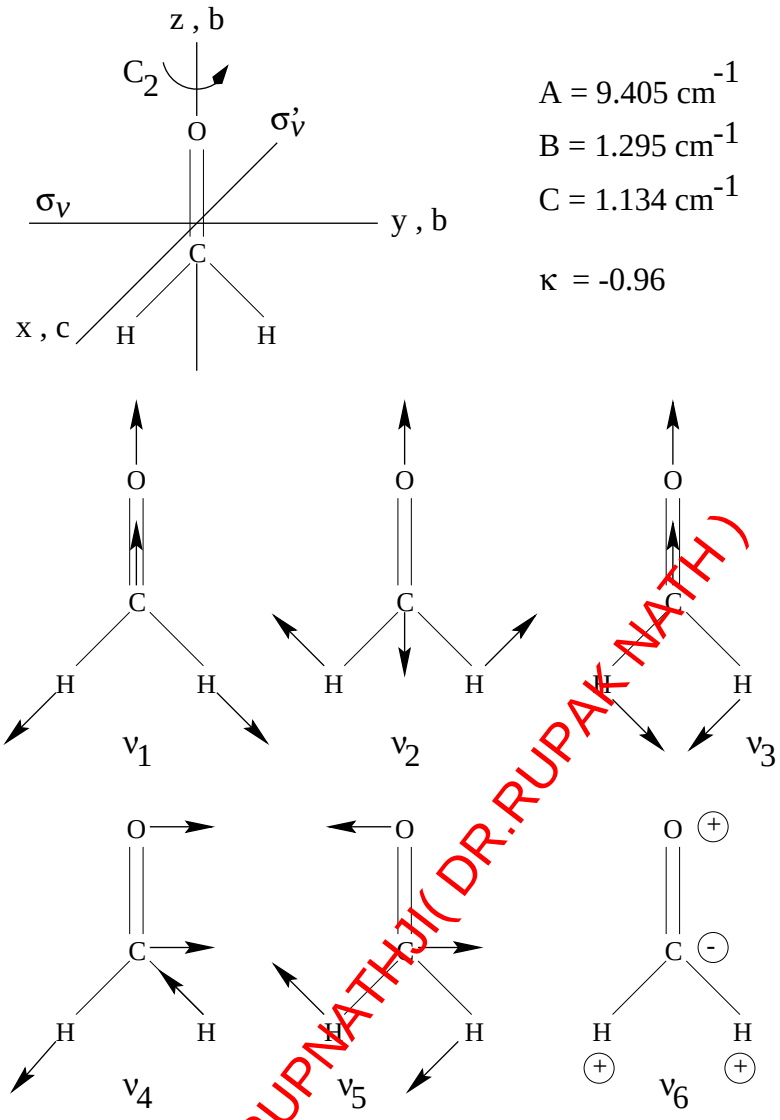

Figure 10.13– The structure and vibrational normal modes of formaldehyde.

What are the symmetries of the normal modes? Clearly, the C_{2v} symmetry of the molecule is maintained in the ν_1, ν_2, and ν_3 modes, and so they are all A_1. The ν_6, or out-of-plane bending, mode, is B_1, and the remaining ν_4 and ν_5 modes are B_2. The ν_1, ν_2, and ν_3 modes have dipole derivatives that change along the a-axis, and so these vibrational transitions are A-type bands with $\Delta K_p = 0$ and $\Delta K_o = \pm 1$. They thus look much like symmetric top perpendicular bands, with symmetric PQR profiles at low spectral resolution. For ν_4 and ν_5, the $\Delta\mu$ is along the b-axis, and they have $\Delta K_p = \pm 1$ and $\Delta K_o = \pm 1$. ν_6 has $\Delta\mu$ along the c-axis, and so is of C-type with $\Delta K_p = \pm 1$, $\Delta K_o = 0$. These latter B- and C-type bands are, as before, very messy with no easily noticeable structure by the untrained eye...

Formaldehyde: Electronic Structure and Spectroscopy

The molecular orbtials involved with the low-lying electronic states of formaldehyde

are all associated with the valence electrons in the carbonyl group. If we ignore the "core" $1s$ orbitals on H, C and O, then there are six $2p$ electrons left to account for. The molecular orbitals associated the carbonyl group are classified as σ and σ^*, π and π^*, and n (the * are for anti-bonding orbitals, and the n is for non-bonding). A pictorial outline of these orbitals is presented below:

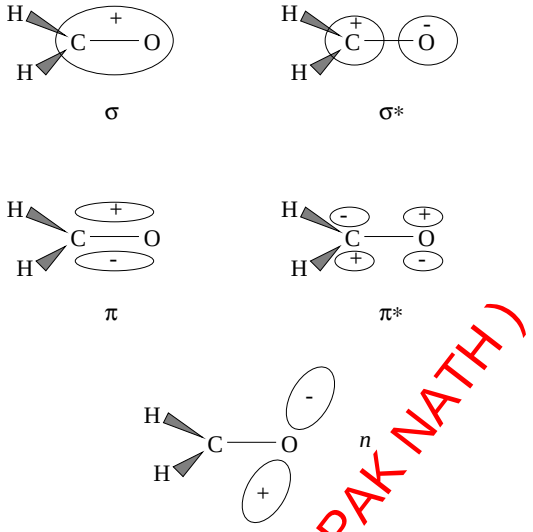

Figure 10.14– The molecular orbital structure of the valence electrons of formaldehyde.

What are the C_{2v} symmetries of these orbitals? By examining the properties of each under the various symmetry operations [for example, under the C_2 operation the σ and σ^* orbitals are unchanged (and are hence of a symmetry), while the π, π^*, and n all change sign (and are hence of b symmetry)], we find the symmetry properties and orbital occupancy outlined next:

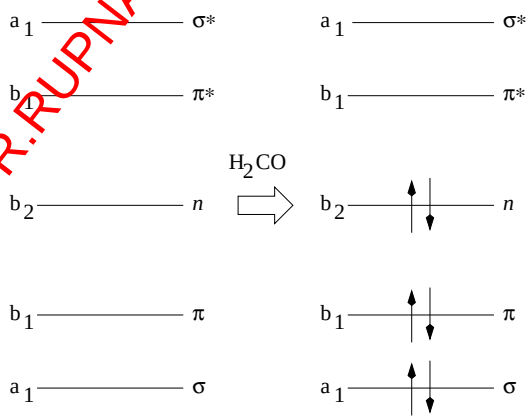

How do we obtain the symmetry of the ground and excited electronic states? For the ground state, the configuration is $\sigma^2\pi^2n^2$, and so the symmetry is

$$\sigma^2\pi^2n^2 \quad = \quad a_1^2b_1^2b_2^2 \quad = \quad a_1a_1a_1 \quad = \quad A_1 \quad .$$

(The individual orbitals are labeled with lower case letters since the capitals are needed for the overall wavefunctions).

What is the lowest electronic transition? Clearly, from the orbital diagram above it is the $n \rightarrow \pi^*$ transition. What is the symmetry of the upper state? Using the same arguments as above, the π^* state has a configuration $\sigma^2\pi^2 n\pi^*$ and so

$$\sigma^2\pi^2 n\pi^* \quad = \quad a_1^2 b_1^2 b_2 b_1 \quad = \quad A_2 \quad .$$

Is this an allowed transition? Remember that the matrix element $< \psi' | \mu | \psi'' >$ must be totally symmetric. From the C_{2v} character table we have that x, y, z are A_1, B_1, B_2. Since the ground electronic state is A_1, this means that ψ' must be $A_1, B_1,$ or B_2. Thus, for $n \rightarrow \pi^*$,

$$< A_2 | \mu(A_1, B_1, B_2) | A_1 > \quad \neq \quad A_1$$

and so the transition is *not* electric dipole allowed.

What about other low-lying transitions?

$$\pi \rightarrow \pi^* \quad \Rightarrow \quad a_1^2 b_1^2 b_1 b_1 \quad \text{so} \quad A_1 \rightarrow A_1 \qquad \text{allowed, by z} - \text{component of } \mu$$

$$n \rightarrow \sigma^* \quad \Rightarrow \quad a_1^2 b_1^2 b_2 a_1 \quad \text{so} \quad A_1 \rightarrow B_2 \qquad \text{allowed, by y} - \text{component of } \mu$$

Although these latter two bands are electric dipole allowed, and intense, there are no discrete spectra because all the lines are *lifetime broadened* by photophysical and photochemical processes (more next time).

The $n \rightarrow \pi^*$ actually shows up weakly, and since it is the longest wavelength transition is actually diagnostic of carbonyl groups (just as the weak 2800 cm^{-1} C–H stretch in aldehydes is diagnostic of that group). Why? Basically, it is due to the breakdown of the Born-Oppenheimer approximation. In reality, the amount of vibrational excitation and its character does in fact slightly change the electronic wavefunction. Perturbation theory then tells you that other electronic states must be mixed in, with the degree of mixing being related to the matrix element between the states divided by their energy separation. Such electric dipole forbidden transitions that gain their intensity in this manner are called **vibronically allowed**.

For example, in H_2CO the ground state electronic wavefunction is A_1, so if any single vibration is excited the overall wavefunction has that character (ignoring rotation). To some (small) extent, therefore, the overall wavefunction gains the character of the vibrational wavefunction. For the $n \rightarrow \pi^*$ transition in formaldehyde, it is observed that the b symmetry vibrations create intensity, while the a symmetry bands do not. Further, the bands show a marked sensitivity to the polarization state of the radiation. Does this make sense? Let's look first at μ_z in the limit where we can still use the symmetry products for the electronic and vibrational parts of the wavefunction, that is:

$$< \phi'_e \phi'_v | \mu_z | \phi''_e \phi''_v > \quad = \quad < A_2 \phi'_v | a_1 | A_1 a_1 > \quad = \quad 0$$

for all vibrations in the $^1A_2$ excited electronic state and transitions from the ground electronic and vibrational state. However, consider next μ_y:

$$< \phi'_e \phi'_v | \mu_y | \phi''_e \phi''_v > \quad = \quad < A_2 \phi'_v | b_1 | A_1 a_1 > \quad = \quad ?$$

For $\phi'_v = \nu_6$, the vibrational symmetry in the upper state is b_1, and $b_1 A_2 b_1 = A_1$, and so group theory says the transition is allowed. The *strength* of the transition depends on the magnitude of the breakdown of the Born-Oppenheimer approximation.

We might expect the spectrum to contain a series of bands like

$$2_0^v 6_0^1 \quad ,$$

where the notation means $\nu_6 = 0 \rightarrow 1$ and $\nu_2 = 0 \rightarrow v$. The different values of v are called a *progression* in the electronic transition (if $\Delta v = 0$, a *sequence* is defined by the different values of v that give rise to the bands). What governs the intensity distribution with v? Just as for the diatomic case, it is the Franck-Condon factors. Life gets more complicated because we are now dealing with a multi-dimensional potential energy surface, and so the change in geometry (hence the extent of the progressions in the Franck-Condon factors) can occur along several normal mode coordinates. In addition, the rotational sub-structure in the bands of the $n \rightarrow \pi^*$ transition is complicated because a variety of selection rules apply since formaldehyde in the excited state is no longer planar.

What does the $n \rightarrow \pi^*$ transition in formaldehyde look like? The next page presents two kinds of spectra of this transition. The first is an absorption spectrum from the ground state that reveals long progressions in the ν_2 and ν_6 modes (in the figures, the mode labeled ν_4 is that called ν_6 by Herzberg). From the diagrams at the beginning of the lecture, we see that these modes involve a carbonyl stretch and the out-of-plane bend. What does this tell us? The fact that the out-of-plane $0 \rightarrow 3$ bending transition is as intense as that for $0 \rightarrow 1$ means that the A_2 state is *non-planar* (it is, in fact, bent by approximately 32°). The long progression in ν_2 means that the bond C–O bond length changes, which is not too surprising since we are exciting to an anti-bonding orbital on the carbonyl chromophore. Not much else is 'lit-up", and so changes in the other degrees of freedom must be minimal.

The lower spectra is that of the fluorescence after excitation of the $4_0^1 3_0^1$ transition in the π^* state. Whereas the absorption spectrum revealed long progressions of vibrational modes in the excited state, here the long progressions are to vibrational modes *in the* $X^1 A_1$ *state*. This is one of the real advantages of electronic spectroscopy. When sharp features are present, the rovibrational structure in absorption can be used to probe the upper state potential while that in emission can be used to look at the ground state rovibrational eigenvalues. It is therefore possible to acquire a great deal of information about the force field in the molecule from a single spectrum, when acquired with sufficient resolution.

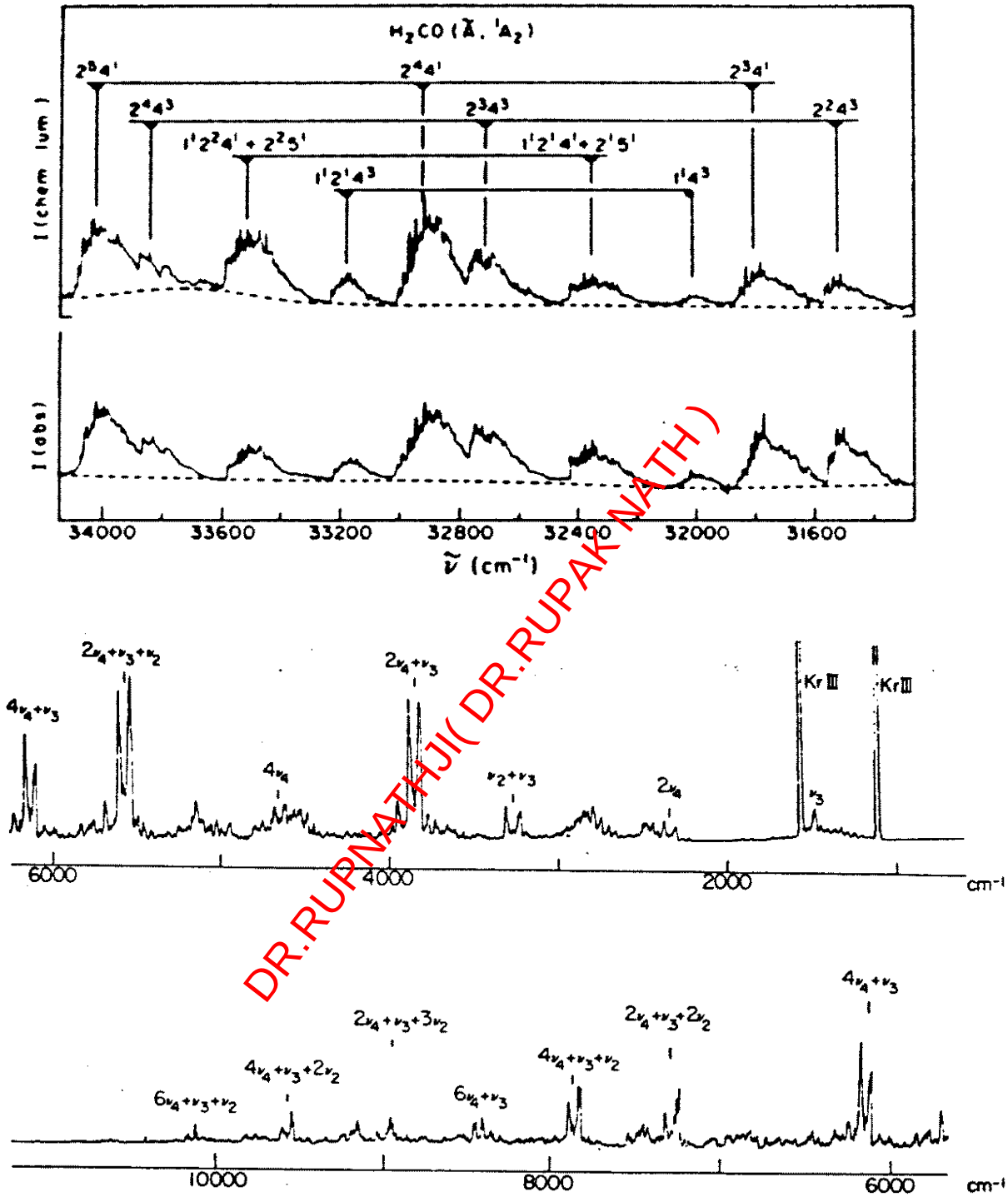

Figure 10.15– (Top) The absorption spectrum of the $n \rightarrow \pi^*$ transition of H_2CO at 6 cm^{-1} resolution. The various vibrational progressions in the $^1A_2$ state are labeled for clarity. (Bottom) The dispersed fluorescence spectrum from H_2CO after excitation of the $X\ ^1A_1 \rightarrow 4_0^1 3_0^1\ A\ ^1A_2$ transition at 3375 Å. The horizontal axis gives the displacement in cm^{-1} from the exciting line, and the vibrational assignments now correspond to the levels on which the fluorescence terminates *in the ground electronic state*.

6. Electronic Spectroscopy and Non-Radiative Processes

As was noted briefly above, the ultraviolet spectroscopy of formaldehyde (specifically the $\pi \rightarrow \pi^*$ and $n \rightarrow \sigma^*$ transitions) is complicated by the fact that at 3 eV or more of excitation the spectral lines are broadened by processes which limit the lifetime of the excited state. The energetics for the photochemical processes in H_2CO are outlined in the figure below:

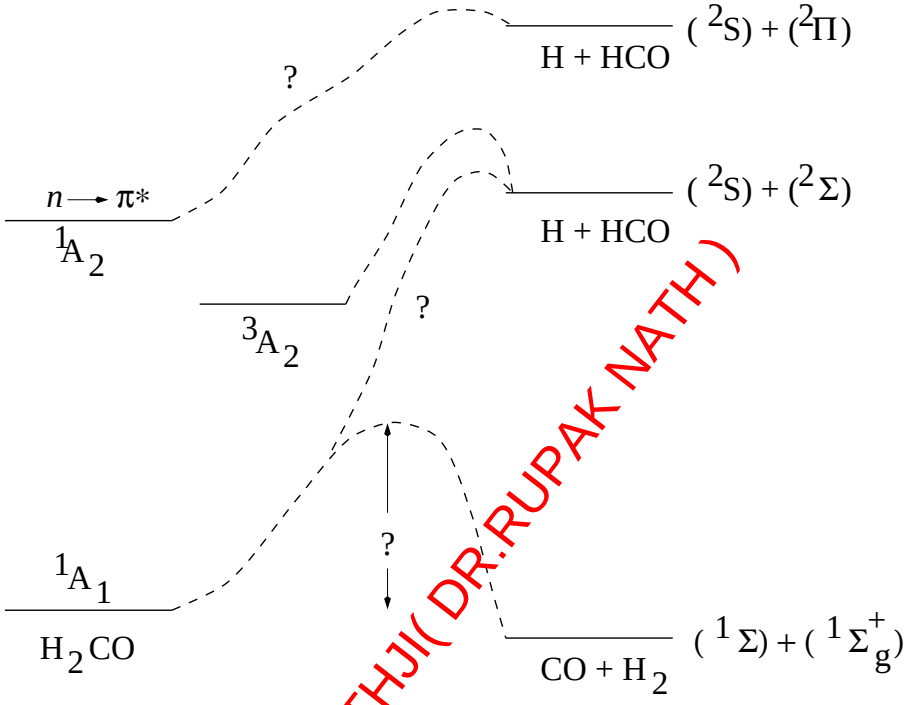

Figure 10.16– The photochemical energetics for formaldehyde photodissociation.

A major question in how fast the various photodissociation processes can occur is the nature of the barriers involved. That is, what are the barriers to the photochemical production of H_2 + CO or H + HCO from formaldehyde? The energetics are easy to lay out, but if large activation energies are involved then it may take photons of considerably greater energy to drive the photochemistry. Other questions concern the nature of singlet-triplet coupling (i.e. is the $^3A_2$ state involved in the decay of $^1A_2$?), etc.

Studies of the isolated benzene molecule in the late 1960's also raised a number of interesting questions. It was found, for example, that if the fluorescence yield (that is, the number of photons emitted/number of molecules excited) from the excitation into the first excited singlet state was examined as a function of pressure in a static cell, even at very low pressures only about 20% of the molecules excited actually emitted photons. Stranger still, if the fluorescence yield was examined as a function of vibrational energy content in the A state, the yield started at 20% and then dropped sharply toward zero above an excitation energy of 39,682 cm^{-1}. These results are summarized in Figure 10.17 below. The fact that the fluorescence yield was well below zero, and changed rapidly with excitation, was cited as a "breakdown of quantum mechanics" by the research teams involved!

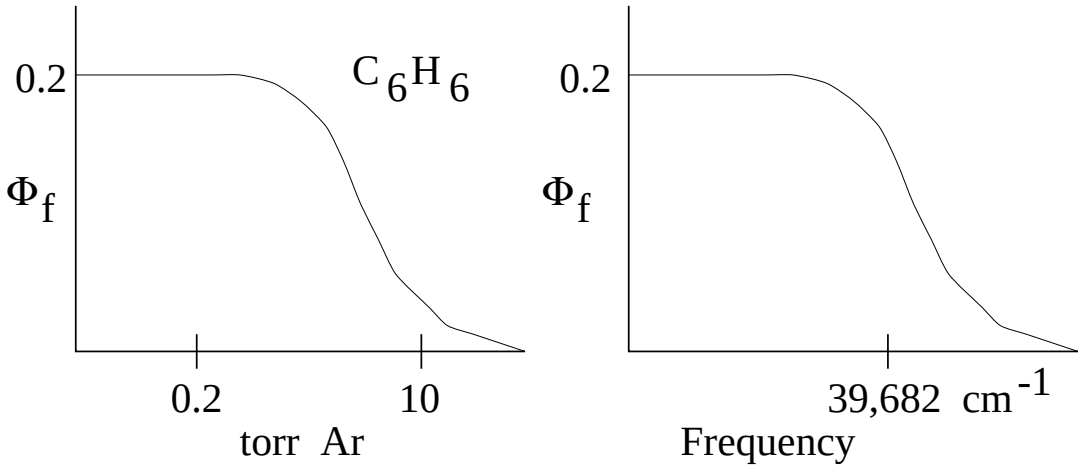

Figure 10.17– (Left) The fluorescence yield from the S_1 state of benzene as a function of background gas (in this case, Ar) pressure. Even at very low pressures the quantum yield is $\ll 1$ [*J. Chem. Phys.* **51**, 1982(1969)]. (Right) The fluorescence yield from the S_1 state of benzene as a function of internal energy in the S_1 state. The rapid drop in emission above a certain threshold energy was called the "channel three problem," and working this problem out contributed greatly to our understanding of energy flow in isolated molecules [*J. Chem. Phys.* **46**, 674(1967)].

This drop in fluorescence yield is now understood to arise from non-radiative processes which operate even on isolated molecules once their density of states becomes sufficiently high. Pictorially, we use plots of the electronic state energies shown below, called Yablonski diagrams, to illustrate the competition between radiative and non-radiative processes in the energy flow within molecules after electronic excitation. Figure 10.18 below outlines the "kinetic rates" at which processes such as fluorescence, internal conversion, etc. occur, while Figure 10.19 stresses the important role that high lying vibrational states play in many of these processes, especially those of internal conversion and intersystem crossing.

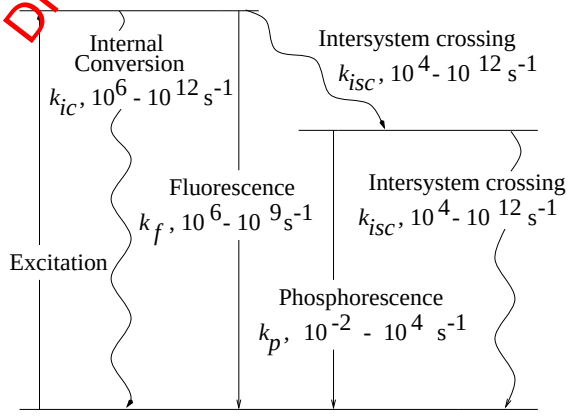

Figure 10.18 A summary of the radiative (→) and non-radiative processes – along with their rates – in electronic spectroscopy.

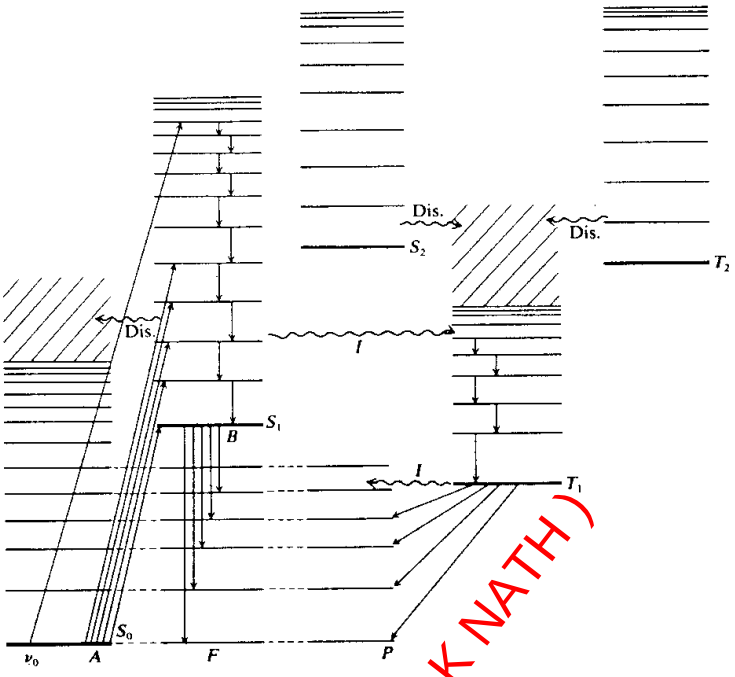

Figure 10.19 The role of vibrational excitation and state density in the balance between radiative ($\rightarrow$) and non-radiative processes after electronic excitation.

The quantum yield for fluorescence can thus be written as

$$\Phi_f = k_f / \sum_i k_i \quad ,$$

where i runs over all the possible radiative and non-radiative processes that can occur. Those include:

k_f = fluorescence (spin, dipole allowed, relatively fast)
k_p = phosphorescence (spin, forbidden, typically slow for low z)
k_{ic} = internal conversion (non – radiative transfer in the same spin manifold)
k_{isc} = intersystem crossing (non – radiative transfer to different spin manifolds)

The lifetime of the upper state, τ_f, is determined by all of the processes,

$$\tau_f = 1 / \sum_i k_i \quad ,$$

and so the quantum yield may be re-expressed in the form

$$k_f = \Phi_f / \tau_f \quad .$$

Consistency checks for the presence of fast, non-radiative processes can be performed by checking the magnitudes of the Einstein A and B coefficients. For purely radiative processes, the relationships derived in §III.1 are valid, but the effective value of A will

be much larger if processes such as internal conversion and/or intersystem crossing occur. We'll next look at simple two versus three level modes of radiationless processes.

The Douglas Effect

Consider the two cases outlined in Figure 10.20 below. On the left we have a simple two level system. For such a system, the fluorescence yield must be unity, that is $\Phi_f = 1$, and all the photons one expect are radiated (there is no place else for the energy to go). Thus, $c_1(t)^2 \; + \; c_2(t)^2 \;\; = \;\; 1$.

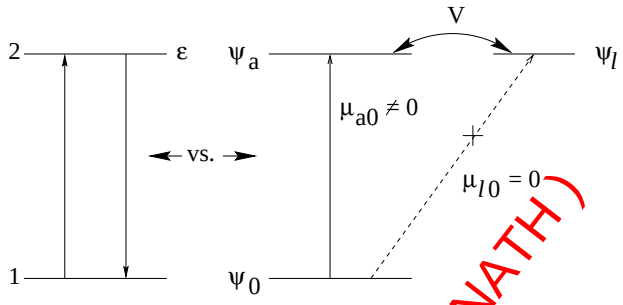

Figure 10.20 The simplest quantum mechanical model of radiationless processes. On the left is a simple two-level system. Non-radiative processes are included by adding a third level, degenerate with the upper state, for which the electric dipole matrix element with the lower state is zero (right).

Life gets more interesting when a third level is added, as is shown on the right of Figure 10.20. Let us suppose that, for a given $\hat{H}_\circ$, the upper states are degenerate, that is

$$\hat{H}_\circ|\psi_a> \;\; = \;\; \epsilon|\psi_a> \qquad \text{and} \qquad \hat{H}_\circ|\psi_l> \;\; = \;\; \epsilon|\psi_l> \;\; .$$

Suppose further it is possible to pump to ψ_a, that is the $0 \rightarrow a$ transition is allowed, but that the $0 \rightarrow l$ transition is forbidden (the H atom is one such system). ψ_a is called the *bright state*, and ψ_l the **dark state**.

Now, turn on a perturbing, or interaction, Hamiltonian $\hat{H}'$ with strength V. Degenerate perturbation theory tells us the energies of the two states in the full Hamiltonian $\hat{H}_\circ + H'$ are given by

$$\begin{vmatrix} \varepsilon & V \\ V & \varepsilon \end{vmatrix} = \varepsilon \pm V \quad \Rightarrow \quad \begin{array}{ll} |+> & \varepsilon + V \\ & \quad 2V \\ |-> & \varepsilon - V \end{array}$$

with wavefunctions of the form

$$|-> \;\; = \;\; \sqrt{\frac{1}{2}}[|\psi_a> \; - \; |\psi_l>]$$

$$|+> \;\; = \;\; \sqrt{\frac{1}{2}}[|\psi_a> \; + \; |\psi_l>]$$

Clearly, *both* of the $|0> \rightarrow |-> $ and $|0> \rightarrow |+>$ transitions are now allowed, at least formally. Let's consider two limiting cases for $t = 0$, one in which $|\varphi(0)> = |\varphi(+)>$, and one in which $|\varphi(0)> = |\psi_a>$.

(A) t = 0; let $|\varphi(0)> = |\varphi_+>$. In a real system, this would mean using a laser whose bandwidth $\Delta\omega$ was such that $\Delta\omega < 2V$. Since $|\varphi(+)>$ is an eigenstate of the total Hamiltonian, we have

$$\hat{H}\varphi_\pm \quad = \quad \epsilon_\pm\varphi_\pm \quad = \quad (\epsilon \pm V)\varphi_\pm \quad .$$

The time dependence for φ_+ is

$$\Phi(t) \quad = \quad U(t)\varphi_+(0) \quad = \quad e^{-i\hat{H}t/\hbar}\varphi_+(0) \quad = \quad e^{-i\omega_+ t/\hbar}\varphi_+(0) \quad ,$$

where $\omega_+ \ = \ (\epsilon + V)/\hbar$. Thus, we see that φ_+ is a stationary state of the system since

$$|\Phi(t)|^2 \quad = \quad |\varphi_+(0)|^2 \quad .$$

The same is true, of course, for φ_-

(B) t = 0; let $|\varphi(0)> = |\varphi_a> = [|\varphi_+> + |\varphi_->]/\sqrt{(2)}$, that is, suppose we prepare only the bright state φ_a which is composed of equal parts φ_+ and φ_- (which requres a laser with $\Delta\omega > 2V$). In this case,

$$|\Phi(t)|^2 \quad = \quad |e^{-i\hat{H}t/\hbar}[\varphi_+(0) + \varphi_-(0)]/\sqrt{(2)}|^2 = \quad \frac{1}{2}[|\varphi_+|^2 + |\varphi_-|^2 + \varphi_+^*\varphi_- e^{-i\Delta\omega t} + c.c.] \quad ,$$

where $c.c.$= complex conjugate (of the third term), and $\Delta\omega = \omega_+ \ - \ \omega_- \propto 2V$. Thus, because ψ_a is not an eigenstate of the full Hamiltonian the probability for finding the system in the ψ_a bright state, which is the one that fluoresces and hence is observable experimentally, oscillates; and the stronger the interaction matrix element V the faster the oscillation is. This in turn induces an uncertainty in the energy which is proportional to the splitting. Since the fluorescence is related to the probability distribution, which is given by

$P_a(t) = [1 + \cos(4\pi Vt/h)]/2 \Rightarrow$

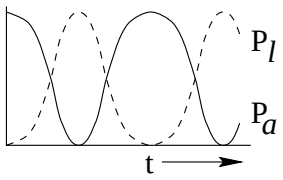

where the so-called *recurrence time* is found to be $\tau = \pi\hbar/V$.

The fluorescence decay is simply

$$\text{Fluorescence} \quad \sim \quad \frac{dP}{dt} \quad = \quad |<\psi_{ex}|\mu|\psi_{gnd}>|^2 \frac{4\omega^3}{3c^3\hbar} \quad .$$

Suppose the excited state is written in terms of the ψ_a and ψ_l states discussed above, or

$$\psi_{ex} \quad = \quad \alpha(t)\psi_a \ + \ \beta(t)\psi_l \quad .$$

We can rewrite the above and find that

$$\frac{dP}{dt} \quad = \quad |\alpha(t)|^2 |\mu_{0a}|^2 \frac{4\omega^3}{3c^3\hbar} \quad ,$$

since $|\mu_{0l}| = 0$. Clearly, the experimentally measured lifetime must be longer (that is, the decay rate slower) since

$$|\mu_{0a}|^2_{effective} \quad = \quad |\alpha(t)|^2 |\mu_{0a}|^2 \quad < \quad |\mu_{0a}|^2 \quad .$$

This is called the **Douglas effect**.

(C) Suppose there are *many* $|l>$ dark levels. For a pure continuum the probability of recurrence into $|a>$ is extremely small. Thus, the Douglas effect transforms into an *irreversible* non-radiative process (much like photodissociation) when the density of vibrational states becomes large. This is illustrated in Figure 10.21. The energy uncertainty is defined by the spread of the quasi-continuous $|l>$ states. In general, this process of randomization of vibrational energy from a bright initial state to a range of dark states that are more or less statistical in nature is called Intramolecular Vibrational Energy Redistribution, or IVR, and its rate can be roughly calculated using Fermi's Golden Rule. In small molecules at low vibrational state densities IVR is slow, but for molecules as large as benzene or larger, the IVR timescales can be of order picoseconds or faster.

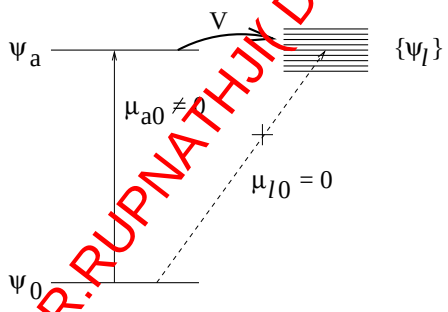

Figure 10.21 An outline of IVR, where the irreversible non-radiative process is driven by the high rovibrational state density of the dark $|l>$ levels.

For the process of InterSystem Crossing, or ISC, the coupling occurs between singlet ($|a>$) and triplet ($|l>$) levels (or in general, between any two different spin manifolds, singlet-triplet, doublet-quartet, etc.). How does this take place?

Spin-Orbit Coupling in Molecules

In the Born-Oppenheimer approximation, the full wavefunction is written as a product of spatial and spin terms. If σ_g and σ_T are the ground and excited triplet state spin wavefunctions, then

$$^1S_0 \ \rightarrow \ ^3T_1 \quad \Rightarrow \ < \varphi_g \sigma_g |\mu| \varphi_T \sigma_T > \ = \ < \varphi_g |\mu| \varphi_T >< \sigma_g | \sigma_T > \ = \ 0$$

due to the orthogonality of the spin wavefunctions. However, the spin-orbit term

$$\hat{H}' \quad \propto \quad \sum_i \mathbf{L_i} \cdot \mathbf{S_i}$$

can couple the excited state singlets and triplets (that is, the normal states we draw in the Yablonski diagrams are *not* the true eigenstates of the total Hamiltonian, just as the $|nl>$ states alone are not the true eigenstates of the hydrogen atom)!

In the perturbed basis set, perturbation theory tells us the the true triplet wavefunction should be written

$$\Psi_{triplet} \quad = \quad \alpha\varphi_T\sigma_T \quad + \quad \beta\varphi_s\sigma_s \quad ,$$

and that the phosphorescence rate is thus related to

$$< \Psi_{ground}|\mu|\Psi_{triplet} > \quad = \quad \alpha < \varphi_g\sigma_g|\mu|\varphi_T\sigma_T > \quad + \quad \beta < \varphi_g\sigma_g|\mu|\varphi_s\sigma_s > \quad .$$

The first term is zero, but the second is not, and so

$$\text{Phosphorescence} \quad \propto \quad |\mu_{gs}|^2\beta^2 \quad ,$$

where $\beta \sim H'_{s.o.}/\Delta E$. In these formulae, $|\mu_{gs}|$ is the singlet-singlet dipole coupling matrix element, and since it is (or can be) non-zero, the triplet lifetime is finite. The spin-orbit matrix element, $H'_{s.o.}$ is often of order 0.1 cm^{-1} for compounds involving first- or second-raw atoms, while ΔE, the electronic state energy separation, is more typically 10^4 cm^{-1}. Thus, triplet lifetimes are some $(10^5)^2$ times longer than that for singlet-singlet fluorescence for most molecules. However, if heavy atoms are involved (such as V- or Os-containing porphyrins that are found in the environment), the spin-orbit coupling is much larger and the phosphorescence yield can be much larger.

ISC in H_2CO

As a quantitative example of how intersystem crossing occurs, let's look at the relatively simple case of formaldehyde. As we saw before, for the $n \rightarrow \pi^*$ excitation, the $^1n\pi^*$ configuration has A_2 symmetry in its spatial wavefunction. For singlets, the spring function has a_1 symmetry, while for the triplets the three spin wavefunctions have a_2, b_1, and b_2 symmetry. Thus, the symmetry of the singlet and triplet manifolds of formaldehyde have the symmetries outlined in Figure 10.22. Let S_x, T_y be given triplet states. As always, for an interaction to occur we demand that the interaction matrix element be of A_1 symmetry, that is

$$< S_x|\hat{H}_{s.o.}|T_y > \quad \equiv \quad A_1$$

for the case of intersystem crossing. Since the spin-orbit interaction is a scalar, it is clearly of A_1 symmetry. Thus, for formaldehyde (and by inference other C_{2v} species as well), the singlet and triplet states must have at least one shared symmetry type for the coupling to be finite. For example:

	Singlet Symm.		Triplet Symm.	Interaction?
$n \rightarrow \pi^*$	$^1A_2$	$n \rightarrow \pi^*$	$^3A_1$, $^3B_1$, $^3B_2$	No
$\pi \rightarrow \pi^*$	$^1A_1$	$n \rightarrow \pi^*$	$^3A_1$, $^3B_1$, $^3B_2$	Yes
$n \rightarrow \sigma^*$	$^1B_2$	$n \rightarrow \pi^*$	$^3A_1$, $^3B_1$, $^3B_2$	Yes
$\pi \rightarrow \pi^*$	$^1A_1$	$\pi \rightarrow \pi^*$	$^3A_2$, $^3B_1$, $^3B_2$	No
	.		.	
	.		.	
	.		.	

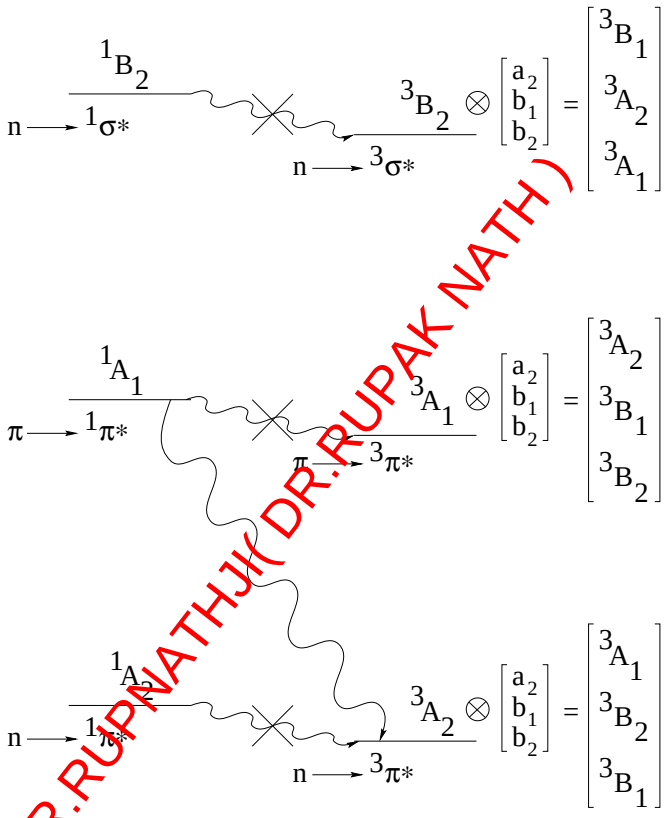

Figure 10.22 An outline of the potential singlet-triplet coupling in formaldehyde driven by the spin-orbit interaction. Arrows denote states that are coupled, those with crosses cannot interact by symmetry.

The interactions outlined above can be generalized, in that for C_{2v} molecules singlets and triplets of the *same configuration* ($n\pi^*$, etc.) do **not** interact, those from different configurations do. Again, the spin orbit matrix element is of order $\hat{H}_{s.o} \sim 0.1$ cm^{-1}, or about 3 GHz. In this case, the appropriate level spacing (the ΔE above) is of the same order since it is the rovibrational states that are coupled, not isolated vibrations. Thus, the time scale for ISC is similar to that for fluorescence or even faster, that is $\tau_{ISC} \leq 10^{-9}$ sec. So, we expect the coupling to be fast and irreversible even for isolated molecules! This is how the UIR features outlined in §IX are formed.